



Published in final edited form as:

Int J Radiat Oncol Biol Phys. 2020 April 01; 106(5): 1063–1070. doi:10.1016/j.ijrobp.2019.12.013.

Evaluating Positron Emission Tomography-Based Functional Imaging Changes in the Heart After Chemo-Radiation for Patients With Lung Cancer.

Yevgeniy Vinogradskiy, PhD^{*}, Quentin Diot, PhD^{*}, Bernard Jones, PhD^{*}, Richard Castillo, PhD[†], Edward Castillo, PhD[‡], Jennifer Kwak, MD[§], Daniel Bowles, MD^{||}, Inga Grills, MD[‡], Nicholas Myziuk, PhD[‡], Thomas Guerrero, MD, PhD[‡], Craig Stevens, MD[‡], Tracey Scheffter, MD^{*}, Laurie E. Gaspar, MD, MBA^{*}, Brian Kavanagh, MD, MPH^{*}, Moyed Miften, PhD^{*}, Chad Rusthoven, MD^{*}

^{*} Department of Radiation Oncology, University of Colorado School of Medicine, Aurora, Colorado

[†] Department of Radiation Oncology, Emory University, Atlanta, Georgia

[‡] Department of Radiation Oncology, Beaumont Health System, Royal Oak, Missouri

[§] Department of Radiology, University of Colorado School of Medicine, Aurora, Colorado

^{||} Rocky Mountain Regional VA Medical Center, Aurora, Colorado

Abstract

Purpose: Studies have noted a link between radiation dose to the heart and overall survival (OS) for patients with lung cancer treated with chemoradiation. The purpose of this study was to characterize pre- to posttreatment cardiac metabolic changes using fluorodeoxyglucose/positron emission tomography (FDG-PET) images and to evaluate whether changes in cardiac metabolism predict for OS.

Methods and Materials: Thirty-nine patients enrolled in a functional avoidance prospective study who had undergone pre- and postchemoradiation FDG-PET imaging were evaluated. For each patient, the pretreatment and posttreatment PET/CTs were rigidly registered to the planning CT, dose, and structure set. PET-based metabolic dose-response was assessed by comparing pretreatment to posttreatment mean standardized uptake values (SUV_{mean}) in the heart as a function of dose-bin. OS analysis was performed by comparing SUV_{mean} changes for patients who were alive or had died at last follow-up and by using a multivariate model to assess whether pre- to posttreatment SUV_{mean} changes were a predictor of OS.

Results: The dose-response curve revealed increasing changes in SUV as a function of cardiac dose with an average SUV_{mean} increase of 1.7% per 10 Gy. Patients were followed for a median of 437 days (range, 201–1131 days). SUV_{mean} change was significantly predictive of OS on multivariate analysis with a hazard ratio of 0.541 (95% confidence intervals, 0.312–0.937). Patients alive at follow-up had an average increase of 17.2% in cardiac SUV_{mean} while patients that died had an average decrease in SUV_{mean} decrease of 13.5% ($P = .048$).

Corresponding author: Yevgeniy Vinogradskiy, PhD; yevgeniy.vinogradskiy@ucdenver.edu.

Supplementary material for this article can be found at <https://doi.org/10.1016/j.ijrobp.2019.12.013>.

Conclusions: Our data demonstrated that posttreatment SUV changes in the heart were significant indicators of dose-response and predictors of OS. The present work is hypothesis generating and must be validated in an independent cohort. If validated, our data show the potential for cardiac metabolic changes to be an early predictor for clinical outcomes.

Summary

The importance of the heart has been highlighted for lung cancer patients receiving radiotherapy. Our study characterized pretreatment to posttreatment positron emission tomography (PET) changes in the heart. The data showed a dose-response curve and that PET changes in the heart were predictive of overall survival. PET imaging is frequently obtained for lung cancer patients and if validated by independent studies, our data show the potential for PET cardiac changes to be an early predictor for clinical outcomes.

Introduction

Studies have highlighted the clinical impact of the radiation dose to the heart for patients with lung cancer receiving radiation therapy.^{1,2} There has been a noted link between radiation dose to the heart and 3 clinical outcomes: (1) overall survival (OS),^{2,3} (2) cardiotoxicity,⁴ and (3) lung toxicity.⁵ Patients who receive higher radiation doses to the heart are likely to (1) have decreased OS,² (2) increased probability of cardiotoxicity,^{4,6} and (3) a greater chance of developed pulmonary side effects, which can include radiation pneumonitis.^{5,7} Multivariate analysis from a Radiation Therapy Oncology Group dose escalation study for patients with non-small cell lung cancer (NSCLC; study #0617) showed that increased heart doses (volume of heart receiving 40 Gy [V40]) were significantly associated with decreased OS.²

Studies across multiple disease sites and clinical endpoints (OS and normal tissue toxicity) have demonstrated that factors beyond dose-volume can improve prediction of clinical outcomes. In particular, it has been shown that functional imaging can improve prediction of both OS⁸ and toxicity.^{9,10} In the domain of cardiac imaging, investigators have used functional imaging to assess cardiac dose-response in patients with breast cancer^{11–14} and patients with esophageal cancer.¹⁵ The cardiac functional imaging assessment has been accomplished using Doppler echocardiography, single-photon emission computed tomography imaging, and ¹⁵O-based positron emission tomography (PET) imaging.^{11–15}

PET imaging using a fluorodeoxyglucose (FDG) radioactive tracer is a standard imaging modality used in the management of lung cancer.¹⁶ PET imaging, and in particular the measurement of FDG uptake with standardized uptake values (SUV), can be used for detection of disease presence, disease staging, and assessment of disease response to treatment. In the setting of radiation oncology, SUV can be used to help delineate gross tumor volume. Although ¹⁸F-FDG-PET computed tomography (PET/CT) imaging has primarily been used to evaluate tumors, studies have suggested that SUV measurements can serve as an inflammatory marker, which can subsequently be used to evaluate the response of normal tissues to treatment.^{10,17–19} FDG-PET imaging is noted as an accepted diagnostic tool to evaluate active cardiac inflammation¹⁸ and has been used to evaluate the response of normal tissue to treatment in the parotid for head and neck¹⁰ treatments, normal lung^{17,19–22}

for lung cancer treatments, and metabolic changes in the heart for patients with esophageal cancer.²³ ¹⁸F-FDG PET/CT imaging is frequently acquired as standard of care for patients with lung cancer but has yet to be evaluated as a means of characterizing and predicting the cardiac metabolic response to thoracic radiation therapy for patients with advanced-stage lung cancer. The purpose of this study was to characterize pre- to posttreatment cardiac metabolic changes using FDG-PET scans and to evaluate whether PET-based cardiac imaging changes predictions for OS.

Methods

Study population

Patients with lung cancer enrolled on a 2-institution, prospective clinical trial for functional avoidance thoracic radiation therapy were analyzed. The study used 4-dimensional CT-based ventilation imaging to reduce dose to functional portions of the lung. The trial hypothesis is that reducing dose to functional portions of the lung will lead to reduced thoracic toxicity rates after chemoradiation. The study was approved to enroll patients by the institutional review boards at the University of Colorado (Aurora, CO) and Beaumont Health System (Royal Oak, MI) ([NCT02528942](#)). Details for the inclusion and exclusion criteria for the clinical trial are previously described.²⁴ Briefly, inclusion criteria included a pathologically confirmed lung cancer diagnosis, a planned concurrent chemotherapy regimen, and a definitive course of photon radiation therapy, which was defined as prescription doses of 45 to 75 Gy. Both patients with NSCLC and patients with small cell lung cancer (SCLC) were enrolled. Patients were excluded if they were treated with stereotactic body radiation therapy (defined as ≤ 5 fractions) or if they received palliative treatment (defined as prescription doses of <45 Gy). Of the patients enrolled on the functional avoidance clinical trial, eligible patients for the present analysis included patients who had completed a pretreatment and a posttreatment PET/CT scan. Thirty-nine patients met the pre- and posttreatment PET/CT imaging criteria and were used for the present study.

Cardiac SUV response analysis

For each patient, the pretreatment PET/CT, posttreatment PET/CT, treatment planning CT, structure set, and dose distribution were imported into MIM Software (MIM Software Inc, Cleveland OH). Using the CT data-set of the PET/CTs, the pre- and posttreatment PET/CTs were rigidly aligned to the treatment planning CT (and were therefore also aligned with the structure set and dose distribution). The registration was done using MIM Software's box-based assisted rigid alignment tool, which performs an automatic rigid fusion using a region of interest selected by the user. The region of interest used for the PET/CT to treatment planning CT registrations was centered on the heart and included the heart, lungs, and a portion of the mediastinum. Each registration was visually reviewed (with particular emphasis on the accuracy of the registration around the heart contour) and adjusted if necessary. The heart contour approved by the clinician for radiation treatment planning was used to evaluate cardiac FDG uptake changes from pre- to posttreatment. The clinically used heart structure was contoured following the Radiation Therapy Oncology Group 1106 guidelines and included the entire heart with the cranial border at the ascending aorta and caudal border at the heart apex. The SUV mean (referred to as SUV_{mean}) and SUV

maximum (referred to as SUV_{max}) were calculated for the heart contour in the pre- and posttreatment PET scans. The SUV_{mean} and SUV_{max} values are reported as mean \pm standard deviation. FDG uptake changes in the heart were calculated as absolute SUV changes and relative percentages (all values are calculated relative to the pretreatment data). A *t* test was used to assess whether the posttreatment cardiac SUV values were significantly different from the pretreatment cardiac SUV. A heart dose-response analysis was performed using previously described dose-response generation methods.^{25,26} The first step was to bin each voxel in the heart contour in to 10 Gy dose bins (range, 0–60 Gy). The SUV_{mean} and SUV_{max} were calculated for voxels in each dose-bin for the pre- and posttreatment PET scans. The pre- to posttreatment SUV differences were then calculated as a function of dose-bin. The dose-response analysis is presented as pre- to posttreatment SUV changes plotted as a function of dose-bin. Linear regression methods were used to determine whether the SUV dose-response slopes were significantly different from zero. In addition to directly comparing pre- to posttreatment SUV values, the cardiac SUV were normalized using liver uptake SUV as previously described^{27,28} to account for potential scanner and patient fasting differences between the pre- and posttreatment PET-CT scans. A sphere of 3 cm in the right lobe of the liver²⁸ was contoured on both the pre- and posttreatment PET-CT scans, and the average SUV were calculated for each sphere. The posttreatment PET scan cardiac values were subsequently scaled by the ratio of the mean pre- to posttreatment liver SUV measurements. The dose-response results using liver SUV normalization are presented in detail in Appendix EA (available online at <https://doi.org/10.1016/j.ijrobp.2019.12.013>) and summarized in the Results section. Studies have shown that in addition to dose to the heart, dose to cardiac substructures (in particular the left ventricle) can be a significant predictor of cardiac outcomes.²⁹ A subanalysis of our data was performed for SUV changes in the left ventricle (LV) and is presented in Appendix AB (available online at <https://doi.org/10.1016/j.ijrobp.2019.12.013>).

Survival analysis

The study assessed whether SUV changes in the heart were predictive of OS. Survival was taken as the time relative to disease diagnosis date. To perform a complete analysis, covariates in addition to SUV changes were considered. Additional covariates available included age, binary status of chronic obstructive pulmonary disease (COPD) presence or absence, disease histology (SCLC vs NSCLC), the volume of the planning target volume, heart dose metrics (mean heart dose, heart V5, V30, V40, V45, and V60), performance status, and disease stage. Univariate and multivariate Cox proportional hazards regression analysis was used to evaluate the effect of SUV, patient, clinical, and treatment factors on OS. Additional analysis was performed by comparing mean cardiac SUV changes and SUV cardiac dose-response curves for patients who were alive or had died at last follow-up. The mean cardiac SUV changes were compared among the surviving and nonsurviving groups using *t* tests and the dose-response curves were compared for the 2 groups using linear regression analysis.

Results

Patient, clinical, and radiation treatment factors for the 39-patient cohort are summarized in Table 1. The median age was 64 (range, 44–84), 49% of patients had preexisting COPD, 92% of patients were current or former smokers, and the median Karnofsky Performance Status was 90 (range, 60–100). The majority (82%) of patients had a NSCLC diagnosis, and 72% of the cohort had stage III disease. Patients were treated with a median dose of 60 Gy (range, 45 Gy to 60 Gy) in 30 fractions (range, 25–30 fractions) with doses per fraction ranging from 1.5 to 2 Gy. The median mean heart dose for the cohort was 11.8 Gy (range, 0.7 Gy to 35.1 Gy). The median time between the last radiation fraction and the posttreatment PET scan was 97 days (range, 11–477 days).

Average SUVmean cardiac values for the pretreatment and posttreatment PET scans were 1.79 ± 0.74 and 1.86 ± 0.97 , respectively ($P = .59$). Similar to the SUVmean results, the SUVmax values were higher for the posttreatment scans (6.56 ± 5.43) compared with the pretreatment PET scans (6.32 ± 4.61 ; $P = .80$). Representative patient examples of a patient with a large decrease in SUV from pre- to posttreatment and a large increase in SUV from pre- to posttreatment are shown in Fig. 1.

A dose-response curve showing the change in pre- to posttreatment SUVmean is presented in Fig. 2. The number of patients contributing to the 0 to 10 Gy, 10 to 20 Gy, 20 to 30 Gy, 40 to 50 Gy, and 50 to 60 Gy dose-bins, were 39 (100%), 38 (97%), 38 (97%), 36 (92%), 36 (92%), and 30 (77%), respectively. The curve displays an overall trend of increasing SUVmean as a function of dose-bin (linear regression $P = 0.055$) with an average increase of 1.7% for every 10 Gy dose bin.

Patients were followed for a median of 437 days (range, 201–1131 days) with 30 of 39 patients alive at last follow-up. COPD status, volume of the planning target volume, mean heart dose, heart V30, heart V40, heart V45, and cardiac SUVmean and SUVmax change were significant ($P < .05$) predictors of OS on univariate analysis. In multivariate analysis, COPD status, heart V40 (the heart V40 was the only heart dose metric chosen for multivariate analysis to avoid collinearity), and the pre- to posttreatment cardiac SUVmean and SUVmax change were predictive ($P < .05$) for OS (Table 2). The hazard ratio for the pre- to posttreatment SUVmean change was 0.541 (95% confidence interval, 0.312–0.937; Table 2).

Figure 3 shows a box-and-whisker plot comparing SUVmean and SUVmax changes for patients who were alive or not-alive at last follow-up. Patients who were alive at follow-up had an average increase of +17.2% in cardiac SUVmean (positive change indicating that posttreatment cardiac SUV is greater than pretreatment cardiac SUV), and patients who had died at last follow-up had an average decrease in SUVmean of -13.5% ($P = .048$). Similarly, patients who were alive at last follow-up had an increase in SUVmax of +47.3%, and patients who were not alive at last follow-up had a decrease in cardiac SUV of -16.2% ($P = .12$). Figure 4 presents dose-response curves grouped according to whether patients were alive or had died at last follow-up. Patients who were alive exhibited increasing change in SUVmean as a function of dose bin ($P = .023$), and patients who were not alive showed

decreasing SUVmean changes as a function of dose bin ($P = .066$). Appendix AC presents Kaplan-Meier survival curves for patients grouped according to cardiac SUVmean changes. The Kaplan-Meier curves show an overall trend of improved OS with increasing SUVmean values. An optimally determined SUVmean threshold of -0.92 was able to significantly ($P = .03$) predict for OS.

The results for cardiac SUV changes normalized to pre- and posttreatment liver SUV are presented in detail in Appendix EA (available online at <https://doi.org/10.1016/j.ijrobp.2019.12.013>). Overall, the results when the data are normalized according to liver SUV are in line with the results using direct cardiac SUV comparisons: a dose-response curve shows increasing SUV as a function of dose (with a slope of 1.4% SUV increase for every 10 Gy dose bin) and SUVmean change was predictive for OS on multivariate analysis (Appendix EA; available online at <https://doi.org/10.1016/j.ijrobp.2019.12.013>).

The results for the LV analysis are presented in detail in Appendix EB (available online at <https://doi.org/10.1016/j.ijrobp.2019.12.013>). The LV data demonstrated a trend of increasing SUVmean as a function of dose-bin (linear regression $P = .028$) with an average increase of 7.0% for every 10 Gy dose-bin. Both the SUVmean and SUVmax changes in the LV were significant (all $P < .05$) in predicting for overall survival on both univariate and multivariate analysis.

Discussion

The overall dose response curve revealed increasing pre- to posttreatment SUVmean changes as a function of dose with an average increase of 1.7% in SUVmean for every 10 Gy. The average SUVmean change in the heart was predictive of OS on both univariate and multivariate analysis. The direction (positive or negative) of change in SUVmean between pre- and posttreatment was significantly different depending on survival status. Patients who were alive at last follow-up demonstrated an increase in pre- to posttreatment SUV (+17.2%) and patients who had died showed a decrease in pre- to posttreatment SUV (-13.5%). Survival status affected the slope and direction of the dose-response curve as patients who were alive had increasing SUVmean cardiac changes as a function of dose, and patients who were not alive had decreasing SUVmean cardiac changes as a function of dose (Fig. 4). FDG-PET scans are most frequently acquired for oncologic staging or evaluation of treatment response.¹⁶ There has been work demonstrating that FDG-PET imaging can also be used to assess cardiac inflammation¹⁸ (it should be noted that fasting and imaging protocols can differ between ¹⁸F-FDG PET/CT oncologic applications and cardiac inflammatory imaging applications) and metabolic viability of the myocardium.³⁰ Studies have demonstrated that cardiac irradiation produces microvascular damage leading to reduced perfusion proportional to the received dose^{12,23,31,32} and that reduced cardiac perfusion corresponds to FDG uptake abnormalities.²³ In this light, one possible mechanistic explanation for the findings in this study is as follows: Radiation causes cardiac microvascular injury³² in proportion to dose leading to local ischemia. The heart responds to the irradiation with metabolic remodeling³³ or enhanced glucose uptake (increase in SUV) within the irradiated myocardium as an adaptive response. Myocardium that is unable to adapt owing to prior disease or to surpassing a critical threshold for damage is ultimately

lost, resulting in a decrease in SUV. Future prospective work with a complete cardiac information data-set is needed to elucidate a complete mechanistic explanation for the presented results.

There has been precedent of using FDG-PET imaging to evaluate treatment response of normal tissues.^{10,17,19–21,34} For head and neck treatments, Roach et al³⁴ showed decreasing FDG uptake in the parotid gland of 5.2% for every 10 Gy (for comparison, the presented cardiac data demonstrated a 1.7% increase for every 10 Gy), and van Dijk et al¹⁰ demonstrated that pretreatment SUV features significantly improved prediction of xerostomia. Guerrero et al¹⁷ characterized the SUV dose-response in the normal lung, and subsequent studies showed that the lung PET-based metabolic response^{20,21} and pretreatment SUV lung features¹⁹ were predictive of symptomatic radiation pneumonitis. Case reports presented^{35,36} have showed increased myocardial FDG uptake after radiation therapy. Using a cohort of patients with esophageal cancer, Jingu et al²³ showed an SUV cardiac response in the irradiated field and demonstrated that SUV increase can correlate with subsequent cardiac magnetic resonance imaging and single-photon emission computed tomography imaging. Similarly, Evans et al showed increased FDG uptake as a function of cardiac dose in patients with early stage lung cancer treated with stereotactic body radiation therapy.²² Our work is in line with previous PET-based, normal tissue studies demonstrating a dose-response and providing evidence that the imaging signal can be predictive of clinical outcomes.

There has been interest in evaluating the role of the heart in thoracic radiation therapy, and our study provides one of the first studies quantitatively characterizing the cardiac PET-based imaging changes in patients with advanced-stage lung cancer (72% of patients had stage III disease). The present work, if validated, provides data suggesting 2 distinct phenotypes with divergent outcomes can be identified with FDG PET imaging; specifically, patients who are at increased risk of death can be identified.

The present study is hypothesis generating, and the results must be validated in an independent, prospective patient cohort. Although the data for the present study was collected on a prospective protocol, the primary aim of the prospective study was not to analyze cardiac SUV changes; as a result, the PET scans were not ideally performed to homogenize the data. The time between pre- and posttreatment PET scans varied, patient diet and fasting conditions for each PET scan may have differed, which can affect cardiac FDG uptake),^{37,38} and no effort was made to perform PET scans on the same scanner for individual patients. Normalization of cardiac SUV to pre- and posttreatment liver SUV was done to mitigate the PET scan variability, as previously described.^{27,28} The consistent results between directly comparing cardiac SUV and data normalized to liver SUV (Appendix EA; available online at <https://doi.org/10.1016/j.ijrobp.2019.12.013>) suggest that the presented data may be durable to variability in PET scan conditions. Although we hypothesize that ¹⁸F-FDG PET/CT presents an inflammatory marker and ¹⁸F-FDG PET/CT has been previously used to evaluate normal tissue inflammation in response to therapy,¹⁷ it should be noted that ¹⁸F-FDG PET/CT scans measuring inflammation have different fasting and imaging protocols¹⁸ than ¹⁸F-FDG PET/CT scans used for oncologic applications.

The dose-response curve in Figure 2 demonstrates that the largest increase in SUVmean occurred in the largest dose-bin (50–60 Gy). Thirty of 39 patients (77%) contributed to the 50 to 60 Gy dose bin. Patient and clinical characteristics were compared among the groups that did and did not contribute to the 50 to 60 Gy dose bin, and only the type of lung cancer (NSCLC vs SCLC) was significantly different ($P < .01$ using the χ^2 test) between the 2 groups. Fewer SCLCs contributed to the largest dose-bin because patients with SCLC were typically prescribed 45 Gy in our study cohort and therefore had lower heart doses than patients with NSCLC. These results suggest that the increase in SUVmean in the largest dose-bin was influenced largely by NSCLC patients.

Our study rigidly registered the PET/CT to the treatment planning CT using methods published in previous dose-response studies.^{15,17} Uncertainty in the registration can manifest in the SUV dose-response curve and may have contributed to the shallow slope of the dose-response (Fig.2). Given that the higher isodose lines were of a relatively low volume in our cohort (Table 1), the registration uncertainty likely had the largest effect on the higher dose-bins. Our data showed that pre- to posttreatment SUV changes were predictive of OS; however, data were not available to analyze whether death was due to cardiac-related events or to assess the effect of pre-existing cardiac comorbidities (heart disease, use of β -blockers). Future studies will focus on an independent, larger cohort validation of the SUV findings presented in the present work. If validated, a clinical trial will be designed to prospectively collect serial PET imaging for patients with advanced-stage lung cancer where PET acquisitions can be standardized and relevant clinical survival data can be collected.

Conclusions

FDG-PET imaging has been used for target delineation and disease response to treatment in thoracic radiation therapy but has yet to be applied to assess cardiac response in patients with advanced-stage lung cancer. The presented study evaluated pre- to posttreatment cardiac SUV changes in patients with advanced stage lung cancer and found increasing SUV as a function of cardiac dose. Pre- to posttreatment cardiac SUVmean change was a significant predictor of OS on multivariate analysis, with patients who were alive at last follow-up demonstrating a +17.2% increase in average cardiac SUV and patients who did not survive showing a –13.5% decrease in average cardiac SUV. Pre- and posttreatment PET imaging is frequently obtained for patients with lung cancer and, if validated by independent studies, the present study's hypothesis generating-data shows the potential for PET cardiac changes to be an early predictor for clinical outcomes.

Supplementary Material

Refer to Web version on PubMed Central for supplementary material.

Acknowledgments

This work was partially funded by grant R01CA200817 (Y.V., J.K., M.M., B.K., E.C., R.C., T.G.).

Disclosures: B.J. discloses an unrelated research grant with Varian Medical Systems.

References

1. Speirs CK, DeWees TA, Rehman S, et al. Heart dose is an independent dosimetric predictor of overall survival in locally advanced non-small cell lung cancer. *J Thorac Oncol* 2017;12:293–301. [PubMed: 27743888]
2. Chun SG, Hu C, Choy H, et al. Impact of intensity modulated radiation therapy technique for locally advanced non-small-cell lung cancer: A secondary analysis of the NRG oncology RTOG 0617 randomized clinical trial. *J Clin Oncol* 2016;35:56–62. [PubMed: 28034064]
3. Stam B, Peulen H, Guckenberger M, et al. Dose to heart substructures is associated with noncancer death after SBRT in stage I–II NSCLC patients. *Radiother Oncol* 2017;123:370–375. [PubMed: 28476219]
4. van Nimwegen FA, Schaapveld M, Cutter DJ, et al. Radiation dose-response relationship for risk of coronary heart disease in survivors of Hodgkin lymphoma. *J Clin Oncol* 2015;34.
5. Huang EX, Hope AJ, Lindsay PE, et al. Heart irradiation as a risk factor for radiation pneumonitis. *Acta Oncologica* 2011;50:51–60. [PubMed: 20874426]
6. Darby SC, Ewertz M, McGale P, et al. Risk of ischemic heart disease in women after radiotherapy for breast cancer. *New Engl J Med* 2013; 368:987–998. [PubMed: 23484825]
7. Dang J, Li G, Ma L, et al. Predictors of grade 2 and grade 3 radiation pneumonitis in patients with locally advanced non-small cell lung cancer treated with three-dimensional conformal radiotherapy. *Acta Oncologica* 2013;52:1175–1180. [PubMed: 23198719]
8. Aerts HJWL, van Baardwijk AAW, Petit SF, et al. Identification of residual metabolic-active areas within individual nslc tumours using a pre-radiotherapy 18fluorodeoxyglucose-PET-CT scan. *Radiother Oncol* 2009;91:386–392. [PubMed: 19329207]
9. Vinogradskiy Y, Castillo R, Castillo E, et al. Use of 4-dimensional computed tomography-based ventilation imaging to correlate lung dose and function with clinical outcomes. *Int J Radiat Oncol Biol Phys* 2013;86:366–371. [PubMed: 23474113]
10. van Dijk LV, Noordzij W, Brouwer CL, et al. ¹⁸F-FDG PET image biomarkers improve prediction of late radiation-induced xerostomia. *Radiother Oncol* 2018;126:89–95. [PubMed: 28951007]
11. Erven K, Jurcut R, Weltens C, et al. Acute radiation effects on cardiac function detected by strain rate imaging in breast cancer patients. *Int J Radiat Oncol Biol Phys* 2011;79:1444–1451. [PubMed: 20605341]
12. Hardenbergh PH, Munley MT, Bentel GC, et al. Cardiac perfusion changes in patients treated for breast cancer with radiation therapy and doxorubicin: Preliminary results. *Int J Radiat Oncol Biol Phys* 2001; 49:1023–1028. [PubMed: 11240243]
13. Marks LB, Yu X, Prosnitz RG, et al. The incidence and functional consequences of RT-associated cardiac perfusion defects. *Int J Radiat Oncol Biol Phys* 2005;63:214–223. [PubMed: 16111592]
14. yromska A, Małkowski B, Wi niewski T, et al. 15o-h2o PET/CTas a tool for the quantitative assessment of early post-radiotherapy changes of heart perfusion in breast carcinoma patients. *Br J Radiol* 2018;91: 20170653. [PubMed: 29470136]
15. Zhang P, Hu X, Yue J, et al. Early detection of radiation-induced heart disease using 99MTC-MIBI spect gated myocardial perfusion imaging in patients with oesophageal cancer during radiotherapy. *Radiother Oncol* 2015;115:171–178. [PubMed: 26072421]
16. National Comprehensive Cancer Network. Non-small cell lung cancer. NCCN guidelines, version 3; 2012.
17. Guerrero T, Johnson V, Hart J, et al. Radiation pneumonitis: Local dose versus ¹⁸[F]-fluorodeoxyglucose uptake response in irradiated lung. *Int J Radiat Oncol Biol Phys* 2007;68:1030–1035. [PubMed: 17398033]
18. Dilsizian V, Bacharach SL, Beanlands RS, et al. ASNC imaging guidelines/SNMMI procedure standard for positron emission tomography (PET) nuclear cardiology procedures. *J Nucl Cardiol* 2016;23:1187–1226. [PubMed: 27392702]
19. Castillo R, Pham N, Castillo E, et al. Pre-radiation therapy fluorine ¹⁸fluorodeoxyglucose PET helps identify patients with esophageal cancer at high risk for radiation pneumonitis. *Radiol* 2015;275:822–831.

20. Hart JP, McCurdy MR, Ezhil M, et al. Radiation pneumonitis: Correlation of toxicity with pulmonary metabolic radiation response. *Int J Radiat Oncol Biol Phys* 2008;71:967–971. [PubMed: 18495373]
21. McCurdy MR, Castillo R, Martinez J, et al. [¹⁸F]-FDG uptake dose-response correlates with radiation pneumonitis in lung cancer patients. *Radiother Oncol* 2012;104:52–57. [PubMed: 22578806]
22. Evans JD, Gomez DR, Chang JY, et al. Cardiac 18F-fluorodeoxy-glucose uptake on positron emission tomography after thoracic stereotactic body radiation therapy. *Radiother Oncol* 2013;109:82–88. [PubMed: 24016676]
23. Jingu K, Kaneta T, Nemoto K, et al. The utility of ¹⁸F-fluorodeoxy-glucose positron emission tomography for early diagnosis of radiation-induced myocardial damage. *Int J Radiat Oncol Biol Phys* 2006;66:845–851. [PubMed: 17011456]
24. Vinogradskiy Y, Rusthoven CG, Schubert L, et al. Interim analysis of a two-institution, prospective clinical trial of 4dct-ventilation-based functional avoidance radiation therapy. *Int J Radiat Oncol Biol Phys* 2018;102:1357–1365. [PubMed: 30353873]
25. Vinogradskiy Y, Diot Q, Kavanagh B, et al. Spatial and dose-response analysis of fibrotic lung changes after stereotactic body radiation therapy. *Med Phys* 2013;40:081712. [PubMed: 23927309]
26. Diot Q, Kavanagh B, Schefter T, et al. Regional normal lung tissue density changes in patients treated with stereotactic body radiation therapy for lung tumors. *Int J Radiation Oncol Biol Phys* 2012;84: 1021–1030.
27. Huang J, Huang L, Zhou J, et al. Elevated tumor-to-liver uptake ratio (TLR) from 18F-FDG-PET/CT predicts poor prognosis in stage IIA colorectal cancer following curative resection. *Eur J Nucl Med Mol Imaging* 2017;44:1958–1968. [PubMed: 28812134]
28. Park J, Chang KJ, Seo YS, et al. Tumor SUVmax normalized to liver uptake on 18F-FDG PET/CT predicts the pathologic complete response after neoadjuvant chemoradiotherapy in locally advanced rectal cancer. *Nucl Med Mol Imaging* 2014;48:295–302. [PubMed: 26396634]
29. Zhang TW, Snir J, Boldt RG, et al. Is the importance of heart dose overstated in the treatment of non-small cell lung cancer? A systematic review of the literature. *Int J Radiat Oncol Biol Phys* 2019;104:582–589. [PubMed: 30630029]
30. Tillisch J, Brunken R, Marshall R, et al. Reversibility of cardiac wall-motion abnormalities predicted by positron tomography. *New Engl J Med* 1986;314:884–888. [PubMed: 3485252]
31. Lauk S, Kiszal Z, Buschmann J, et al. Radiation-induced heart disease in rats. *Int J Radiat Oncol Biol Phys* 1985;11:801–808. [PubMed: 3980275]
32. Yan R, Song J, Wu Z, et al. Detection of myocardial metabolic abnormalities by ¹⁸F-FDG PET/CT and corresponding pathological changes in beagles with local heart irradiation. *Korean J Radiol* 2015; 16:919–928. [PubMed: 26175594]
33. Camici P, Ferrannini E, Opie LH. Myocardial metabolism in ischemic heart disease: Basic principles and application to imaging by positron emission tomography. *Prog Cardiovasc Dis* 1989;32:217–238. [PubMed: 2682779]
34. Roach MC, Turkington TG, Higgins KA, et al. FDG-PET assessment of the effect of head and neck radiotherapy on parotid gland glucose metabolism. *Int J Radiat Oncol Biol Phys* 2012;82:321–326. [PubMed: 21030160]
35. Zöphel K, Hölzel C, Dawel M, et al. PET/CT demonstrates increased myocardial FDG uptake following irradiation therapy. *Eur J Nucl Med Mol Imaging* 2007;34:1322–1323. [PubMed: 17546454]
36. Kawamura G, Okayama H, Kawaguchi N, et al. Radiation-induced cardiomyopathy incidentally detected on oncology 18F-fluorodeoxyglucose positron emission tomography. *Circ J* 2018;82:1210–1212. [PubMed: 28824031]
37. Maurer AH, Burshteyn M, Adler LP, et al. How to differentiate benign versus malignant cardiac and paracardiac 18F FDG uptake at oncologic PET/CT. *Radiographics* 2011;31:1287–1305. [PubMed: 21918045]

38. Cheng VY, Slomka PJ, Ahlen M, et al. Impact of carbohydrate restriction with and without fatty acid loading on myocardial 18F-FDG uptake during PET: A randomized controlled trial. *J Nucl Cardiol* 2010;17:286–291. [PubMed: 20013165]

Author Manuscript

Author Manuscript

Author Manuscript

Author Manuscript

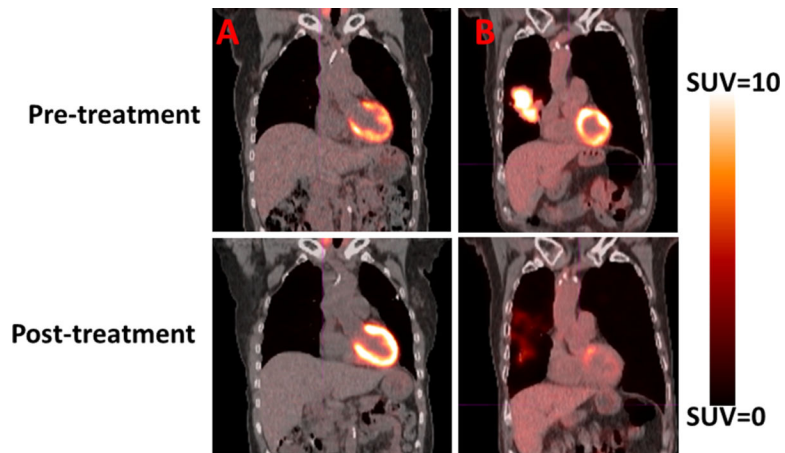


Fig. 1. Pretreatment and posttreatment positron emission tomography/computed tomography scans are shown for 2 patients. (A) The patient presented displayed an increase in posttreatment cardiac standardized uptake values (SUV) compared with pretreatment cardiac SUV. (B) Demonstrated a decrease in posttreatment cardiac SUV compared with pretreatment cardiac SUV.

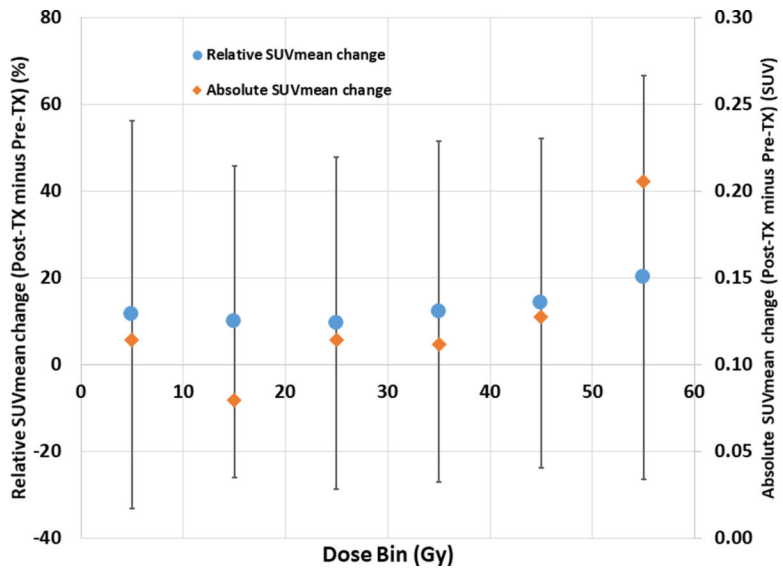


Fig. 2. Change in pretreatment to posttreatment mean standardized uptake values (SUVmean) as a function of dose bin. Both the relative SUVmean changes (scale shown on left) and the absolute SUVmean changes (scale shown on right) are shown. Error bars are presented as standard deviations. For clarity, only error bars for the relative SUVmean series are shown. *Abbreviation:* Tx = treatment.

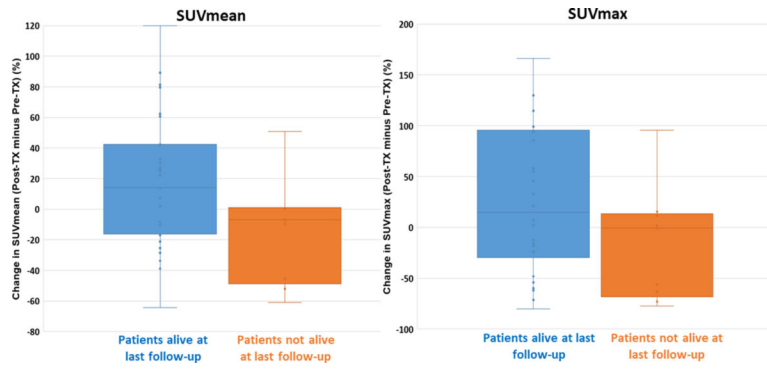


Fig. 3. Box-and-whisker plot comparing pretreatment to posttreatment mean standardized uptake values (SUVmean) and SUVmax changes according to whether patients were alive or not alive at last follow-up. The box-and-whisker plots show the range of values, median values, and 25th and 75th percentiles. *Abbreviation:* Tx = treatment.

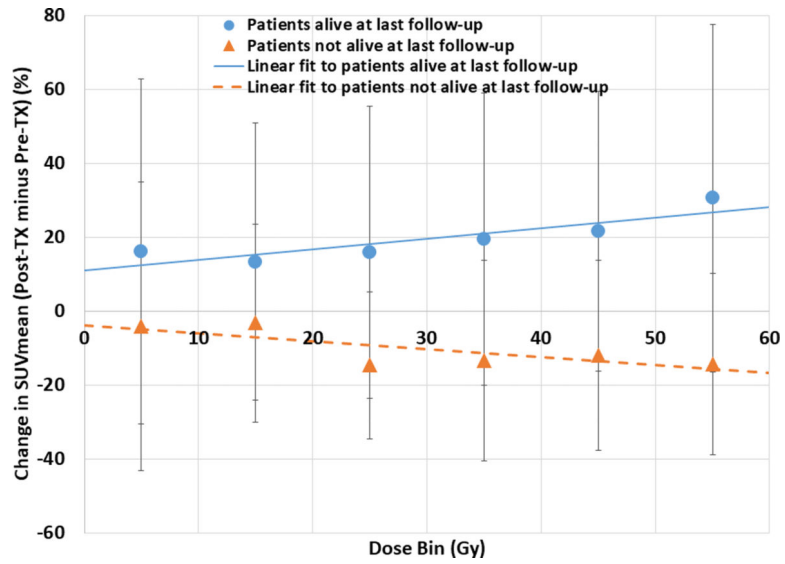


Fig. 4. Change in pretreatment to posttreatment mean standardized uptake values (SUVmean) as a function of dose bin grouped according to whether patients were alive or not alive at last follow-up. Linear regression fits are shown for both groups. Error bars are presented as standard deviations. *Abbreviation:* Tx = treatment.

Table 1

Patient, clinical, and radiation parameters of study cohort.

Parameter	Number (%) or median (range)
Number of patients	39
Gender	
Female	26 (67)
Male	13 (33)
Age	64 (44–84)
COPD	
Yes	19 (49)
No	20 (51)
Smoking status	
Non-smoker	3 (8)
Current smoker	11 (28)
Former smoker	25 (64)
KPS index	90 (60–100)
Type of lung cancer	
NSCLC	32 (82)
SCLC	7 (18)
Stage	
I	2 (5)
II	5 (13)
III	28 (72)
IV	4 (10)
Fractionation	
Total dose (Gy)	60 (45–60)
Number of fractions	30 (25–30)
PTV Volume (cc)	419 (65–1124)
Heart doses	
Mean heart dose (Gy)	11.8 (0.7–35.1)
V5 (%)	48.4 (0.0–100.0)
V30 (%)	9.5 (0.0–65.0)
V40 (%)	5.5 (0.0–39.6)
V45 (%)	4.1 (0.0–25.5)
V60 (%)	0.8 (0.0–8.4)
Time between last radiation treatment and post-treatment PET scan (days)	97 (11–477)

Abbreviations: COPD=Chronic Obstructive Pulmonary Disease, KPS = Karnofsky Performance Status, NSCLC = Non-small cell lung cancer, SCLC = Small cell lung cancer, PTV = Planning Target Volume, V5=Percentage of heart receiving 5 Gy, PET=Positron Emission Tomography

Author Manuscript

Author Manuscript

Author Manuscript

Author Manuscript

Table 2

Parameters predictive of overall survival using the multivariate Cox model.

Covariate	HR (95% CI)	P value
COPD status (binary: COPD not present vs COPD present)	10.623 (2.516–44.855)	0.001
Heart V40 (continuous)	1.109 (1.006–1.223)	0.038
Change in SUV _{Mean} (continuous)	0.541 (0.312–0.937)	0.028
Change in SUV _{Max} (continuous)	0.918 (0.845–0.997)	0.042

Abbreviations: CI = confidence interval; COPD = chronic obstructive pulmonary disease; HR = hazard ratio; Heart V40 = percentage of heart receiving 40 Gy; Change in SUV_{mean} = pretreatment to posttreatment changes in the average cardiac standardized uptake values.

Author Manuscript

Author Manuscript

Author Manuscript

Author Manuscript